Isothermal Crystallization-Induced Phase Transition of Syndiotactic Polystyrene Polymorphism

Rong-Ming Ho,* Chien-Pang Lin, Ping-Yen Hseih, and Tsai-Ming Chung

Department of Chemical Engineering, National Chung Hsing University, Taichung 40227, Taiwan, R.O.C.

Hsien-Yin Tsai

Union Chemical Laboratories, Industrial Technology Research Institute, Hsinchu 30055, Taiwan, R.O.C.

Received April 10, 2001; Revised Manuscript Received June 25, 2001

ABSTRACT: The growth of α and β crystals for melt-crystallized syndiotactic polystyrene (sPS) has been studied by the morphological observations of transmission electron microscopy and the structural analysis of electron diffraction (ED). The crystallographic textures of α and β single crystals were identified by the results of ED and polyethylene decorated experiments. Phase transformation from the α″ phase to the β' phase for bulk and thin film samples was observed during isothermal crystallization. The transition was found to occur in the later stage of crystallization as evidenced by the structural analysis of Fourier transform infrared spectroscopy experiments combined with the enthalpic measurements of differential scanning calorimetry experiments. The coexistent α″ and β' crystals exhibit three specific crystallographic correspondences as identified by the appearance of three different [00*l*] zonal ED patterns. The corresponding diffraction results indicate that the α″ and β' crystals are both grown as flat-on type and possess a common *c*-axis in these structures so as to form dual-layer lamellar texture. The rearrangement of molecular chains during the transition was thus proposed. The initial growth of the metastable α″ crystals is attributed to the kinetic effect of crystallization while the later formation of the β' crystals results from the tendency to reach a thermodynamically more stable state. We suggest that the occurrence of the isothermal transformation is the results of floating chain behavior for sPS crystalline superstructure.

Introduction

Polymorphism of syndiotactic polystyrene (sPS) has been extensively studied in recent years. Structural studies by using X-ray diffraction,[1−8] electron diffraction,[8−14] Fourier transform infrared radiation,[15−23] and solid-state NMR[24−27] have shown a very complex polymorphic behavior for this polymer. Two types of melt-crystallized crystal structures have been identified and described in terms of α and β, both containing the planar-zigzag conformation of backbone chains. The crystalline β form is characterized by orthorhombic chain packing, whereas the crystalline α form is characterized by trigonal chain packing. These melt-crystallized crystalline forms are further complicated by different degrees of structural order. They are two limited disordered modifications, α′ and β', and two limited ordered modifications, α″ and β''.

Recently, the role of metastability in polymer phase transitions has been thoroughly discussed and examined by Keller and Cheng.[28] In addition to classical metastability that describes the phase transformation from one state to another according to the Ostwald stage rule,[29] circumstantial metastability, including morphological, compositional, and other types of metastability, was proposed and believed to be essentially important while the behavior of phase transitions of polymers is discussed. According to this conceptual description of metastability, the metastability of polymorphism may invert with lamellar size where a stable phase defined by the structural metastability can become a metastable phase due to the influence of phase dimensions. This behavior is described as a phenomenon of stability inversion with crystal size.[28,30] Our previous studies have found that the T_m^o (i.e., structural metastability) of the β form in sPS is higher than that of the α form based on the T_m^o determination by using linear Hoffman−Weeks (H−W) extrapolation and nonlinear H−W treatment.[31] The occurrence of phase stability inversion with lamellar size (i.e., morphological metastability) in sPS was recognized (see Figure 14 of ref 31 for details). The origin of the formation of the α″ crystals have been identified as a result of kinetic reason due to the smaller stable size for critical nucleation (i.e., the lower energy barrier required for nucleation). Different pathways of α → b phase transformation can be thus anticipated on the basis of the proceedings of thickening processes. The inceptive α phase may transforms into β phase either during heating or during isothermally crystallization.[31]

In this study, we attempted to explore the possibilities and the related behavior regarding the α → b phase transformation during isothermal crystallization for sPS polymorphic crystals in detail. The behavior of phase transformation is first studied by experimental characterization in the stage of crystal growth. After the inquisition of the possible circumstances for the isothermal transformation, polymorphic sPS single-crystal lamellae are grown and then examined by transmission electron microscopy (TEM). Plausible results with respect to the structural analysis and morphological observations during the transition were obtained in this study. Detailed transformation mechanisms are interpreted on the basis of the crystallographic studies of individual polymorphic crystals as well as the coexistent

* To whom all correspondence should be addressed. Tel 886-4-22857471; Fax 886-4-22854734; e-mail rmho@dragon.nchu.edu.tw.

10.1021/ma010628+ CCC: $20.00
Published on Web 08/15/2001

instances. A unique molecular disposition, floating chain assembly, for the molecular arrangement of sPS crystalline superstructure is thus proposed to explain the occurrence of the phase transformation during isothermal crystallization. Consequently, various molecular rearrangements with respect to different crystallographic types of polymorphic coexistence are proposed in this study.

Experimental Section

Materials. Semicrystalline syndiotactic polystyrene was obtained as courtesy sample materials from Union Chemical Laboratories. The number-average molecular weight of the samples is 67 000 g/mol, and the polydispersity is 3.5. The samples were first dissolved in xylene at 140 °C and then recrystallized in methanol for the purpose of purification.

Differential Scanning Calorimetry (DSC). DSC experiments were carried out in a Perkin-Elmer DSC 7. The temperature and heat flow scales at different heating rates were carefully calibrated using standard materials. The samples were first heated to the maximum annealing temperature, T_{max}, for 5 min in order to eliminate the crystalline residues formed during the preparation procedure of sPS. The polymer samples were then cooled at a rate of 150 °C/min to a preset temperature, T_c, for isothermal crystallization. To study the transformation behavior, the isothermal crystallization was carried out at different isothermal times, t_c. The consecutive heating was performed at heating rate of 10 °C/min. The DSC sample size was around 5 mg for all the melting behavior studies. Each measurement was performed at least twice. Thermal degradation after high-temperature treatment may lead to significant changes in melting behavior.

Fourier Transform Infrared Spectroscopy (FTIR). The sPS powders were hot-pressed to form thin films. The thin film samples were then thermally treated in an Instec STC200 hot stage for different crystallization conditions as previously described. Infrared spectra were obtained via Perkin-Elmer Paragon 500 FTIR at a resolution of 1.0 cm^{-1}. The frequency scale was internally calibrated using a He−Ne laser, and 30−300 scans were signal-averaged to reduce the noise. The scanned wavenumber range was 4000−450 cm^{-1}.

Wide-Angle X-ray Diffraction (WAXD). For WAXD experiments, the same crystallization conditions as described in previous section were carried out on sPS bulk samples. A Siemens D5000 1.2 kW tube X-ray generator (Cu Kα radiation) with a diffractometer was used for WAXD powder experiments. The scanning 2θ angle ranged between 5° and 40° with a step scanning of 0.05° for 3 s. The diffraction peak positions and widths observed from WAXD experiments were carefully calibrated with silicon crystals with known crystal size.

Transmission Electron Microscopy (TEM) and Electron Diffraction (ED). The sPS ultrathin films with thickness in the range of 10 nm for ED experiments were prepared by casting a 0.2% (w/w) sPS and xylene solution onto carbon-coated glass slides. The same crystallization conditions as described in previous section were carried out on the sPS thin film samples. After crystallization, the films were quenched into ice water. The quenched samples were shadowed by Pt and coated with carbon again. After shadowing, the sPS films were stripped and floated onto the water surface and then recovered using copper grids. The ED patterns of sPS were obtained via a JEOL (JEM-1200x) TEM using an accelerating voltage of 120 kV. All of the ED patterns in this study were obtained from selected area aperture around 0.5 μm in diameter. Calibration of the electron diffraction spacing was carried out using Au and TlCl (d-spacing < 3.84 Å, the largest spacing for TlCl). Spacing values larger than 3.84 Å were calibrated by doubling the d-spacings of these reflections.

For the decoration experiments, polyethylene (PE) having narrow molecular weight distribution was vaporized by heating under vacuum (typically, 10^{-4}−10^{-5} Torr) and then crystallized on the fold surface of sPS single lamellar crystals through chain scission.[32,33] The number-average molecular weight of PE in this experiment is around 100 000 g/mol. After decoration, the samples were shadowed by Pt and coated with carbon for TEM observations.

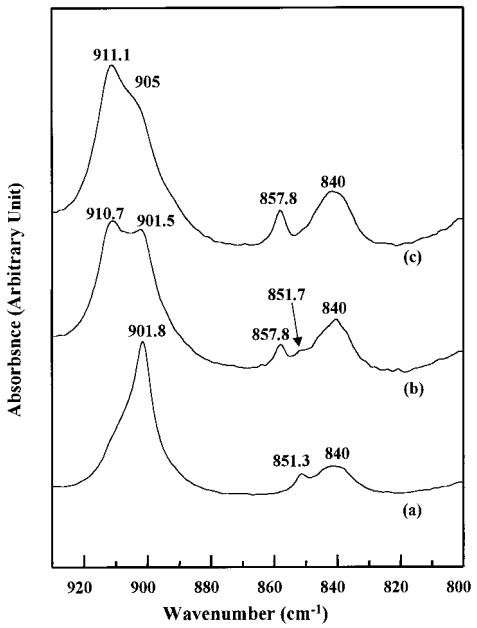

Figure 1. FTIR spectra of sPS crystallized at T_c = 245 °C for (a) t_c = 20, (b) t_c = 40, and (c) t_c = 60 min from the melt (T_{max} = 300 °C).

Results and Discussion

α″ → β′ Phase Transformation. To study the α″ → β′ phase transformation during isothermal crystallization, bulk samples of sPS were isothermally crystallized from the melt at different temperatures for various times. The occurrence of the phase transformation during isothermal crystallization has been evidenced by the structural analysis of FTIR experiments as an example illustrated in Figure 1. The melt-crystallized sample was first grown at 245 °C to form the isolated α″ form where the characteristic fingerprinting absorption of the α″ phase at around 851 and 901 cm^{-1} in FTIR spectra is clearly observed (Figure 1a). Further increasing the isothermal time brings the additional absorption at around 858 and 911 cm^{-1}, which correspond to the characteristic fingerprinting absorption of the β′ phase. Furthermore, the absorption of the α″ phase gradually reduces with time and finally disappears after an extensive annealing. In addition, the absorption at around 905 and 840 cm^{-1} is attributed to the amorphous portions of sPS. Similar results have also been observed by the structural analysis of WAXD experiments. As a result, we suggest that a phase transformation from the α″ → β′ phase occurs during the isothermal crystallization. It is also interesting to find that the amount of the isothermal transformation from the α″ phase to the β′ phase is strongly dependent upon the crystallization temperature. At lower crystallization temperatures, the transformation may not be carried out even after substantially long annealing time. A complete transformation only occurs while the crystallization temperature is above a critical value. These results suggest that the isothermal transformation is pertinent to the temperature-dependent molecular relaxation (see below for reasons).

For crystallization-induced phase transformation, it usually tends to agree that this transformation starts

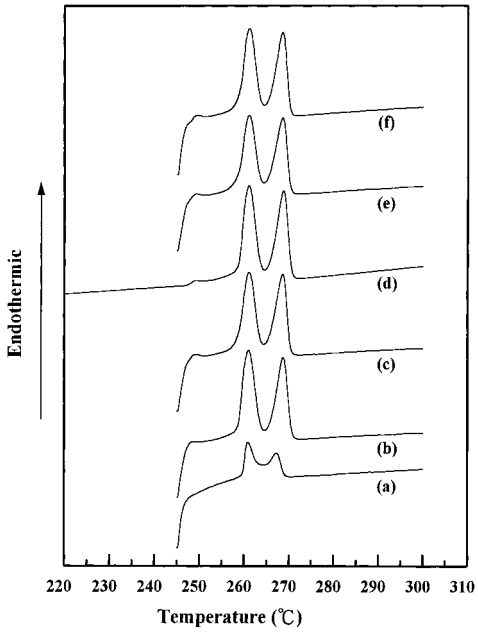

Figure 2. DSC thermograms of sPS crystallized at $T_c = 245$ °C for (a) $t_c = t_p = 2$, (b) $t_c = 4$, (c) $t_c = 20$, (d) $t_c = 20$ (quenched sample), (e) $t_c = 40$, and (f) $t_c = 60$ min from the melt ($T_{max} = 300$ °C).

with a heterogeneous nucleation of an initially grown metastable phase, and a newly formed stable phase later develops through a reorganization and/or recrystallization processes. An important issue regarding the transformation is whether the transformation carries out before the completion of crystallization (i.e., the crystallinity of samples reaches an invariant level). For a transformation before complete crystallization, the behavior of the transition may be described as polymorphic transformations during crystallization processes. For a transformation after complete crystallization, the behavior may be described as the results of annealing. The major difference between these two phenomena is the origins of transformation. The driving force of crystallization is responsible for the isothermal transformation before complete crystallization, whereas the reorganization of molecular chains is responsible for the transformation after complete crystallization. The questions arise with respect to the effects of crystallinity and lamellar thickness of crystallized samples during the transition.

To trace the changes of crystallinity with isothermal conduction time, melt-crystallized sPS samples were examined by DSC measurements (Figure 2). There are arguments about the possibility to form the polymorphism during cooling due to the occurrence of further crystallization so that the FTIR experiments at room temperature may not be a true representation of the in-situ results. In general, the thermograms of DSC measurements were obtained by heating the melt-crystallized samples directly after isothermal crystallization. Contrary to the typical thermograms, the running temperature profile for DSC measurements was carried out from room temperature for quenched samples after crystallization so as to examine the possible changes of crystallinity and/or phase structures during cooling. The comparison result, as shown in Figure 2c,d, excludes the concerns of further crystallization during cooling. The amount of endothermic response (i.e., the sample crystallinity) has been found to be almost invariant when the crystallization time is

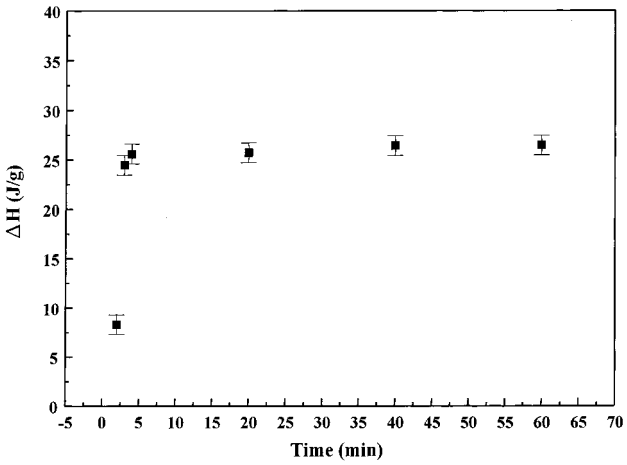

Figure 3. Heat of fusion for sPS crystallized at $T_c = 245$ °C for different isothermal crystallization time from the melt ($T_{max} = 300$ °C).

more than 2 times the exothermic peak time, $t_p = 2$ min, determined from the thermograms of isothermal crystallization (Figure 3). As compared to Figure 2, the time for complete crystallization is obviously shorter than the conduction time required for complete transformation (around 60 min). This indicates that the isothermal $\alpha'' \rightarrow \beta'$ transformation is carried out at an approximately equal level of crystallinity but different lamellar thickness of samples. Further study regarding the lamellar thickness change during transition is under investigation in terms of time-resolved FTIR, WAXD, and SAXS experiments. Nevertheless, the observed results reflect that the isothermal transformation is carried out mainly after complete crystallization.

Crystallography of Polymorphic sPS Single Crystals. To investigate the transition behavior of polymorphic sPS, the growth of single-crystal lamellae was first carried out from melt-crystallized thin film samples. Large single lamellar crystals of polymorphic sPS with micrometer size having smooth surface have been grown from the melt in this study. Figure 4 shows the TEM micrograph and its corresponding ED pattern of the α'' crystals crystallized at 260 °C from the melt for short isothermal time. The assignments of reflections in the ED patterns are obtained in accordance with the trigonal unit cell of α'' crystalline structure proposed by De Rosa[8] and Lotz.[14] The [001] zonal ED pattern suggests that the α'' lamellar crystal grows as a flat-on type with the molecular chains (i.e., *c*-axis) perpendicular to the growing substrate. Furthermore, the α'' single-crystal growth exhibits regularly faceted and hexagonal appearance. The morphological observations are similar to the observed results by Lotz and co-workers.[14] According to the orientation of the corresponding ED results, the growth planes of the faceted lamellae are of {110}. The crystallography of the α'' single-crystal lamellae is thus determined as illustrated in Figure 5a.

In contrast to the shape of the α'' single lamellae grown at short isothermal times, the growth of the β' single lamellae crystallized at 260 °C from the melt after extensive isothermal times exhibits elongated hexagonal appearance (Figure 6a). This result reflects that the isothermal $\alpha'' \rightarrow \beta'$ phase transformation also occurs in sPS thin film samples crystallized at this high temperature. The growth of the regularly faceted β' single crystal in this study exhibits slightly different morphology as compared to the truncated-lozenge appearance

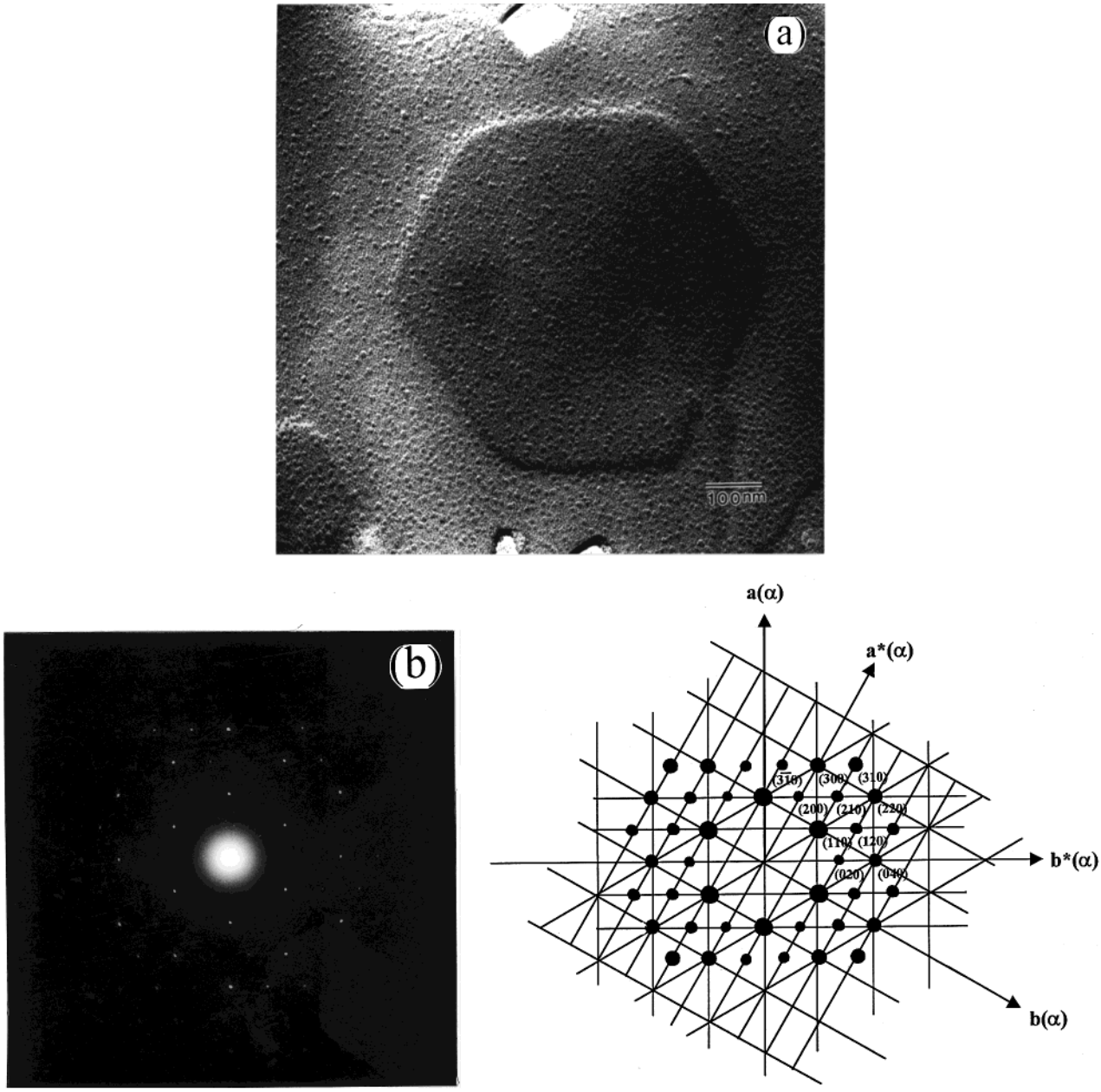

Figure 4. (a) TEM micrograph of α″ crystals crystallized at 260 °C from the melt for 30 min (T_{max} = 300 °C). (b) The ED pattern is obtained from the central area of the micrograph and shown in correct orientation.

of the *β*′ single crystal reported by Tosaka and coworkers.[11] We speculate that the discrepancies are attributed to the various procedures for the growth of single-crystal lamellae. The *β*′ crystals also possess a flat-on type as evidenced by the corresponding [001] zonal ED pattern (Figure 6b). The elongated direction of the single crystal has been identified to be along the *a*-axis of crystal structure. The crystallography of the *β*′ single-crystal lamellae is thus determined as illustrated in Figure 5b. It is noted that the average interplanar angle between the folding planes of short-edged facets is 118°. The long-edged and short-edged growth planes are identified as of the {010} and the {120}. For the α″ lamellar crystals, the interplanar angle of {110} folding plane is 120°. Therefore, the appearance of the *β*′ lamellar crystals is described as an elongated hexagonal shape.

Coexistence of Polymorphic sPS Crystals. The studies of crystallographic textures on polymorphic sPS single crystals indicate that the morphological appearances and the structures of lamellar crystals grown from the melt of thin film samples are strongly dependent upon the isothermal time during the crystallization. After extensive isothermal annealing, the hexagonal α″crystal transforms into the elongated hexagonal *β*′ crystal. To study the transformation mechanism, the thin film samples was isothermally annealed for appropriate time in order to investigate the corresponding structural and morphological changes during the transition. Figure 7a shows one example of our extensive efforts on the morphological observations within the stage of transition. A dual-layer lamellar crystal is identified where the growth of elongated hexagonal lamellae (i.e., the *β*′ crystal) is clearly observed on the top of barely recognized hexagonal lamellae (i.e., the α″ crystal). Surprisingly, a corresponding ED pattern possessing the coexistent (*hk*0) reflections of the α″ and *β*′ single crystals is obtained from this dual-layer crystal as shown in Figure 7b. A specific crystallographic correlation among diffraction vectors of these reflections

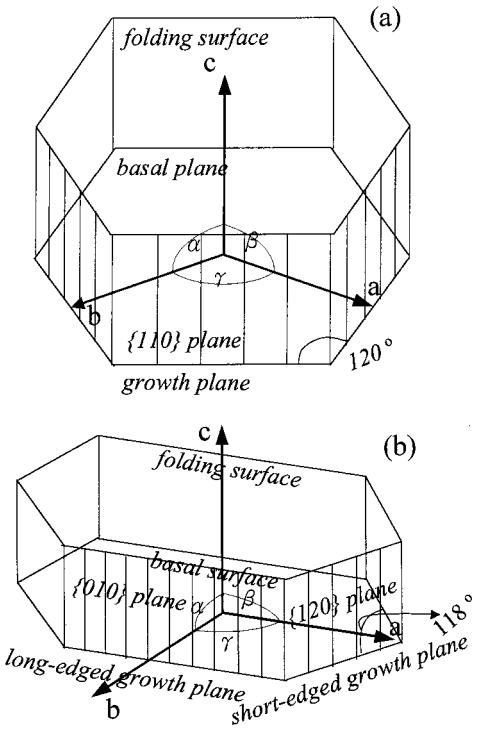

Figure 5. Schematic representation of the lamellar geometry of (a) the α″single crystal and (b) the β′ single crystal.

is found. For example, the diffraction vector of the (120) for this α″ crystal aligns with the diffraction vector of the (0*k*0) reflections of the β′ crystal. Similar results have been found in different prepared samples and sample locations. This observed results suggest that the coexistent α″ and β′ single crystals possess common *c*- and *b*-axes in this crystal structure. We conclude that the formation of dual-layer lamellae is attributed to the phase transformation of the metastable α″ phase (hexagonal shape) to the stable β′ phase (elongated hexagonal shape) on the basis of the observation of morphological contours associated with their structural analyses. In other words, the transformation is indeed to carry out during the thickening process through the rearrangement of molecular chains (see next section for detailed description).

The thickening process is in accordance with the specific crystallographic correlation between the α″ and β′ crystals. Two of symmetrical {110} facets for the α″ phase are transformed into the facets of {010} for the β′ phase, whereas the other {110} facets of the α″ phase become the {120} facets of the β′ phase. In fact, the newly formed {120} planes of β′ phase are almost parallel to the inceptive {110} planes of α″ phase. Figure 7c shows schematic representation of the lamellar crystallography of the coexistent α″ and β′ single crystal.

After examining the crystallized samples during the transition, two other possible specific crystallographic correlation regarding the dispositions of the coexistent polymorphic structures have also been identified. We designate the previous instance as model I for the structural coexistence during the transition. Model II describes a corresponding [001] zonal ED pattern where the diffraction vectors of those (0*k*0) of the α″ crystal and the β′ crystal align each other as shown in Figure 8. This suggests that the coexistent α″ and β′ single crystals possess common *c*- and *a*-axes in this structural orientation. Similar to the morphology observed in model I, the growth of coexistent α″ and β′ crystals also forms a dual-layer lamellae. However, the corresponding shape contours with respect to the growth of two individual crystal forms are difficult to recognize, in particular, the hexagonal shape of the α″ single crystal. We speculate that the indistinct morphology is ascribed to the absence of common orientations with respect to their growth facets. Model III shows that the interangle between the diffraction vectors of (0*k*0) reflections for the α″ crystal and the β′ crystal is around 15° as shown in Figure 9 or around 165° (a mirror image of the previous molecular arrangement). Furthermore, the examined interangle between the diffraction vectors of (0*k*0) reflections is not always exactly 15°. It deviates from this value within 5° variation. The deviation is related to the characteristics of molecular arrangement in model III (see below for reasons). No recognizable morphology with clear facets has been found in this instance.

Proposed Mechanisms for Transformation. As predicted in the phase diagram of stability inversion (see Figure 14 of ref 31), the thickening process during isothermal crystallization gives rise to the tendency of phase transition once the initially crystallized α″ crystals reorganize to form thicker lamellar crystals. The transformation is expected to occur through the shifting of the molecular chains along the *c*-axis during isothermal environment as evidenced by the coexistence of [001] zonal reflections of the α″ and β′ crystals from the dual-layer lamellar morphology. As a result, the reorganization is inevitably relevant to the chain folding dispositions and its conformations. To investigate the fold direction, the lamellae are decorated with PE fragments in terms of the decoration method based on the evaporation and condensation−crystallization of low molecular weight PE molecules.[32,33] No obvious preferred growth orientation of the decorated PE crystal rods is observed on the lamellar surfaces of both phases as shown in Figures 10a,b. Various interpretations for the lack of preferred orientation of PE crystal rods on the fold surface, such as nonuniform folding directions resulting in random orientation of the rod crystals or the formation of irregularly arranged rod crystals resulting from the nontight chain folding conformation, have been proposed. For the crystals of sPS, the complexities of molecular chain packing lead to a variety of structural models proposed by different authors, in particular those for the α phase. The crystal structure of the α phase has been identified as hexagonal structure by Greis and co-workers.[9] The hexagonal packing was further modified as a trigonal, quasi-rhombohedral structure by De Rosa[8] following a succession of several models proposed by Corradini and co-workers.[1,3,4,34] More recently, a frustrated model similar to the model of trigonal structure was also proposed by Lotz and coworkers in order to interpret the complicated molecular arrangements in this superstructure.[14] The major discrepancy of these models is the relative rotation of the so-called triplets, the basic elements for the packing of sPS superstructures, consisting of three molecular chains with the pendent benzene locations in 6-fold symmetry on the *ab*-plane. In the frustrated model of Lotz,[14] the detailed molecular chain packing was proposed by considering azimuthal settings and *c*-axis shifts of the triplets. According to these models and our observed results, we thus hypothesize that these various packing models are the results of loosing chain packing.

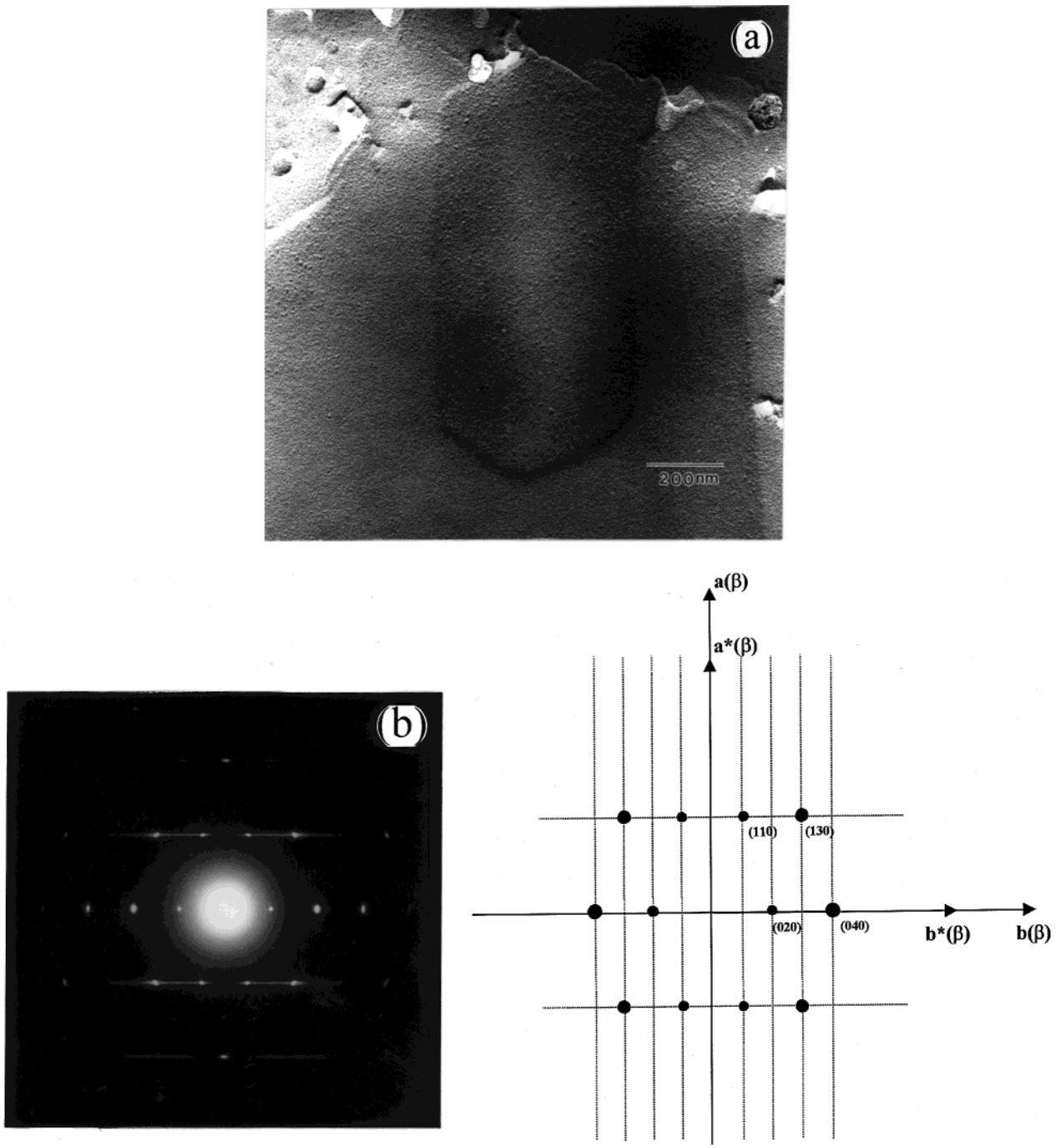

Figure 6. (a) TEM micrograph of β' crystals crystallized at 260 °C from the melt for 180 min (T_{max} = 300 °C). (b) The ED pattern is obtained from the central area of the micrograph and shown in correct orientation.

The molecular chains are more or less like floating segments but assemble to form ordered structure with nontight chain packing. The nontight chain packing in polymorphic sPS crystals forms the less ordered folding surface so that the decorated PE crystal rods are randomly distributed on the folding surface.

To further identify the observed morphology, the decoration experiment has been carried out on the amorphous surface of sPS. There is no apparent texture of the condensation−crystallization of vaporized PE fragments exhibited on the amorphous surface of sPS. This observation provides the means to justify whether the location of decorated area is indeed crystalline area. As shown in Figure 10c, the surface of the dual-layer morphology is decorated by PE crystal rods, whereas no clear decorated texture is observed on the surface of surrounding area (i.e., amorphous area). This result confirms that the dual-layer morphology (Figure 7) corresponds to the lamellar crystals of sPS. The behavior for the transitions are thus proposed as shown in Figure 11a−c with respect to the transition models of I−III, respectively. In these illustrations, the molecular chain is indicated as a simple cylinder projection along the backbone instead of a real projection of chemical structure. This simple scheme, based on the hypothesis of the floating chain packing in the sPS superstructure, ignores the consequence of handed concerns. As a result, we suggest that the hexagonal lattice of the α crystal can be thought to coincide with an orthorhombic point lattice by adjusting the dimensions of *a*- and *b*-axes through the rearrangement of molecular chains along *c*-axis during transition (i.e., the thickening process of

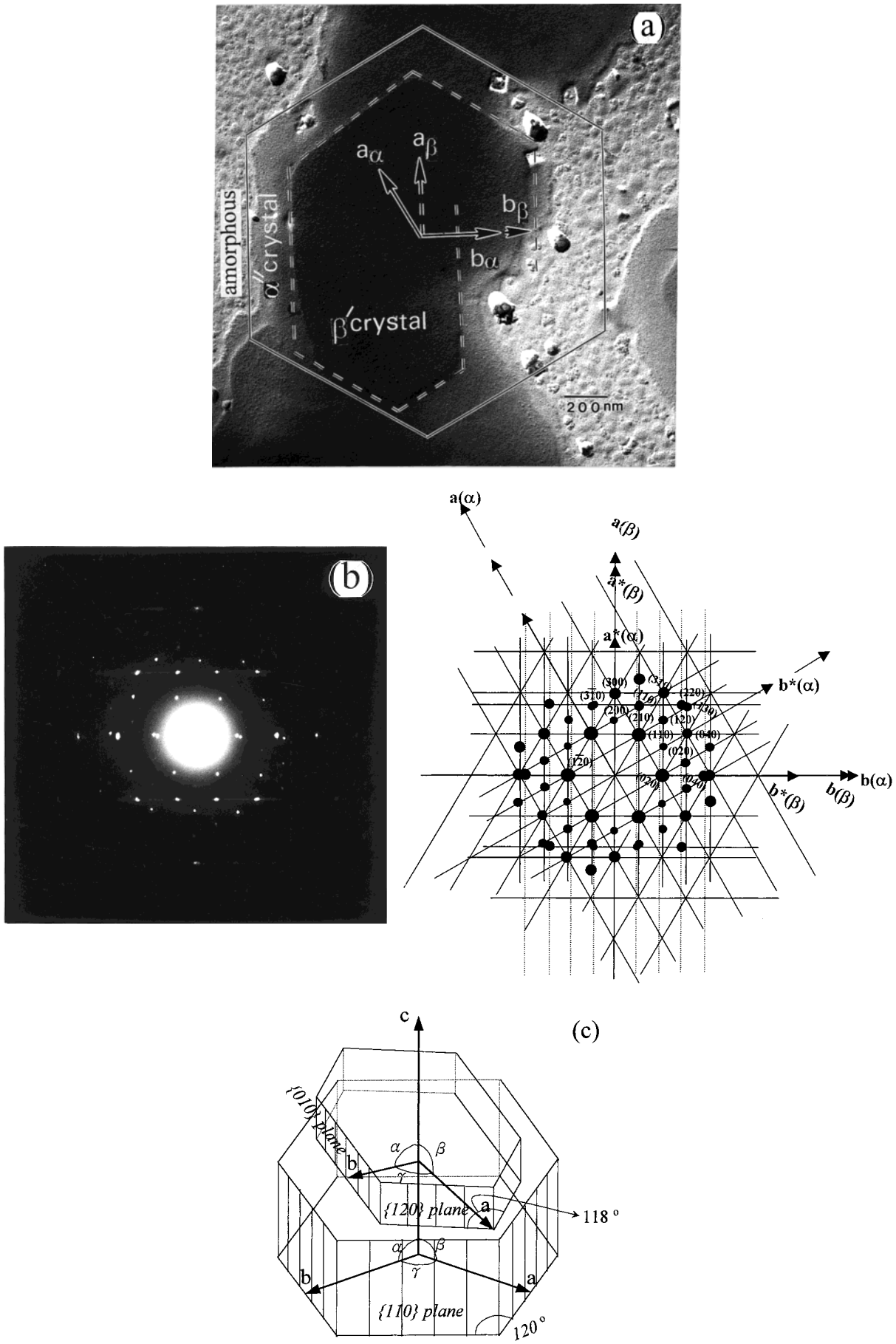

Figure 7. (a) TEM micrograph of coexistent α″ and *β*′ single crystals having common *c*- and *b*-axes (model I) crystallized at 260 °C from the melt. (b) The ED pattern is obtained from the central area of the micrograph and shown in correct orientation. (c) Schematic representation of the lamellar geometry of coexistent α″and *β*′ single crystal for model I.

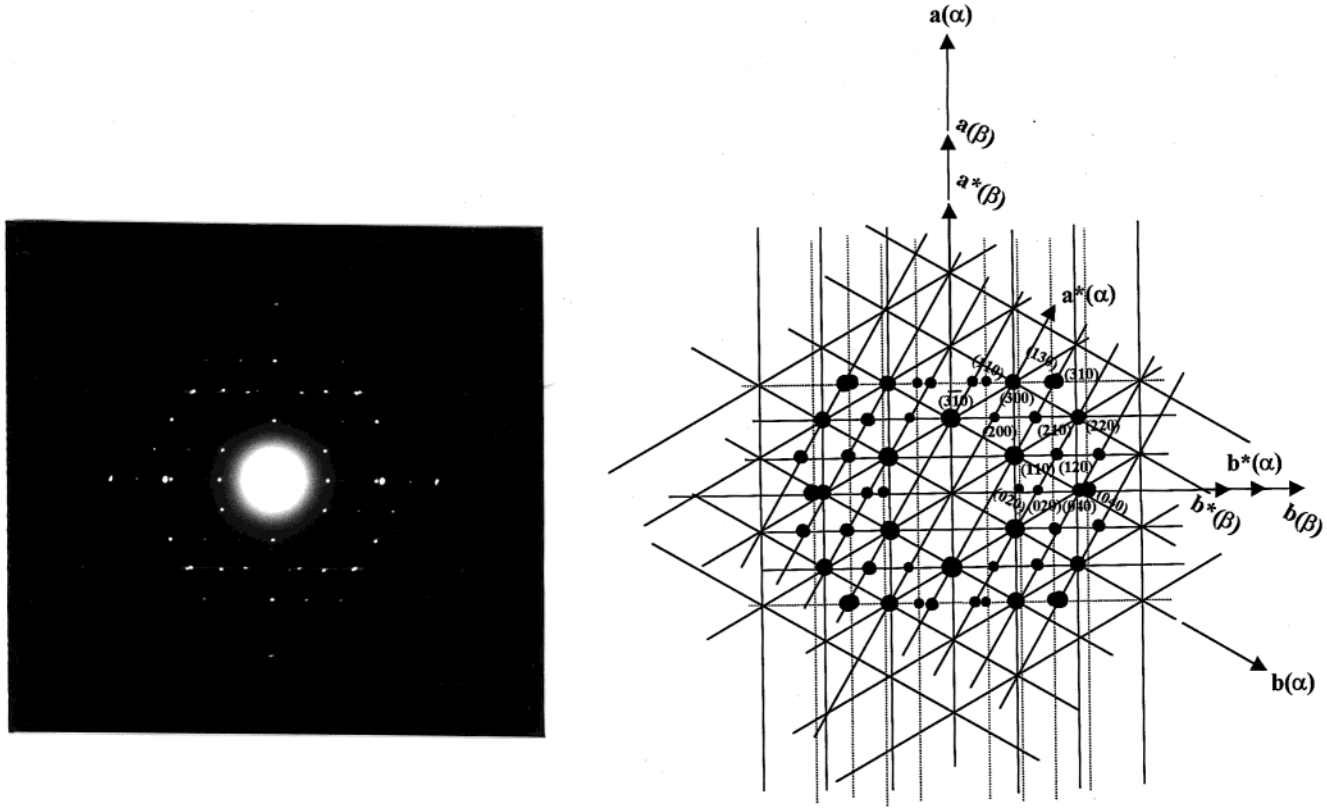

Figure 8. ED pattern of coexistent α″ and β′ single crystals having common *c*- and *a*-axes (model II) crystallized at 260 °C from the melt.

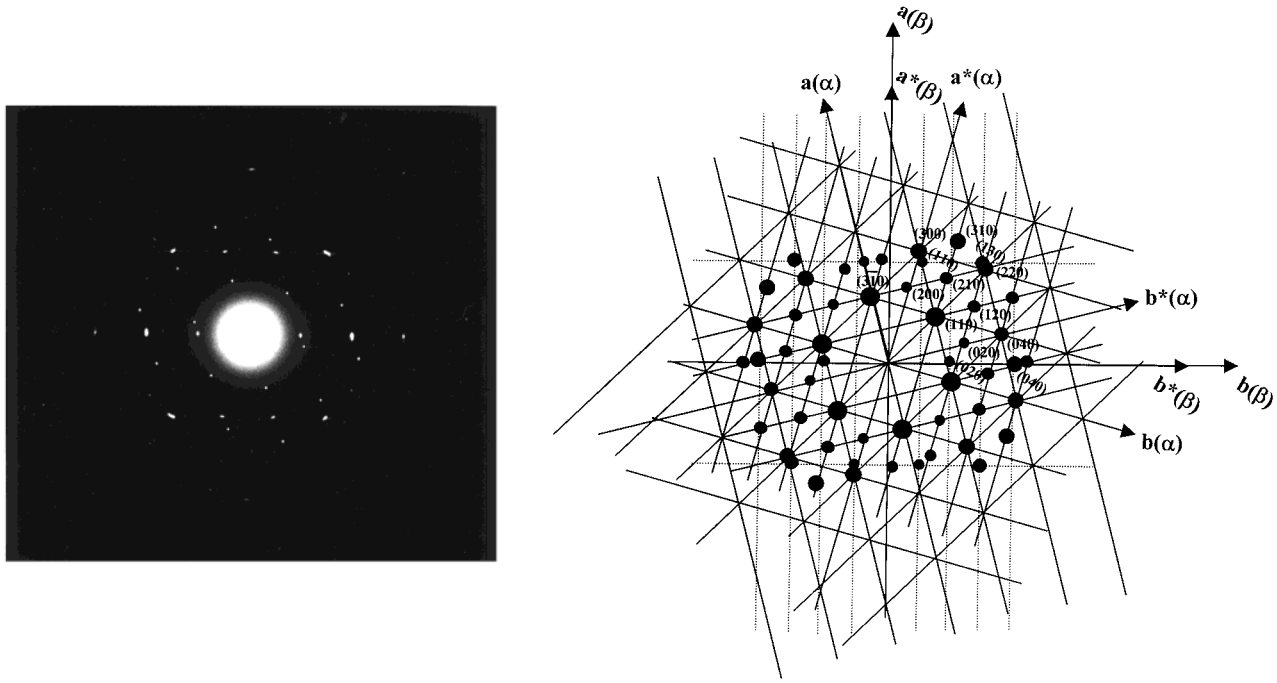

Figure 9. ED pattern of coexistent α″ and β′ single crystals crystallized at 260 °C from the melt where the α″ and β′ crystals possess common *c*-axis and the interangle of their *b*-axes exhibits 15° (model III).

lamellae). Construction of the crystal lattices according to the truly molecular dispositions is thus obtained as shown in the illustrations. Namely, the transformation is achieved by simply aligning the lattice network of α″ phase (open circles with dashed line network) to the lattice network of β′ phase (filled circles with solid line network). The process of alignment is to move the molecular chains of α″ crystals to their closest neighboring positions of the newly formed β′ crystals. For model I, the adjustment of molecular positions from the α″ phase lattice to the β′ phase is inevitable to produce the molecular chain defects (indicated as gray circled area) roughly along the *b*-axis direction of β′ phase (Figure 11a). We suggest that the formation of intermolecular packing defects along the *b*-axis may be one of the possible explanations for the occurrence of streaking

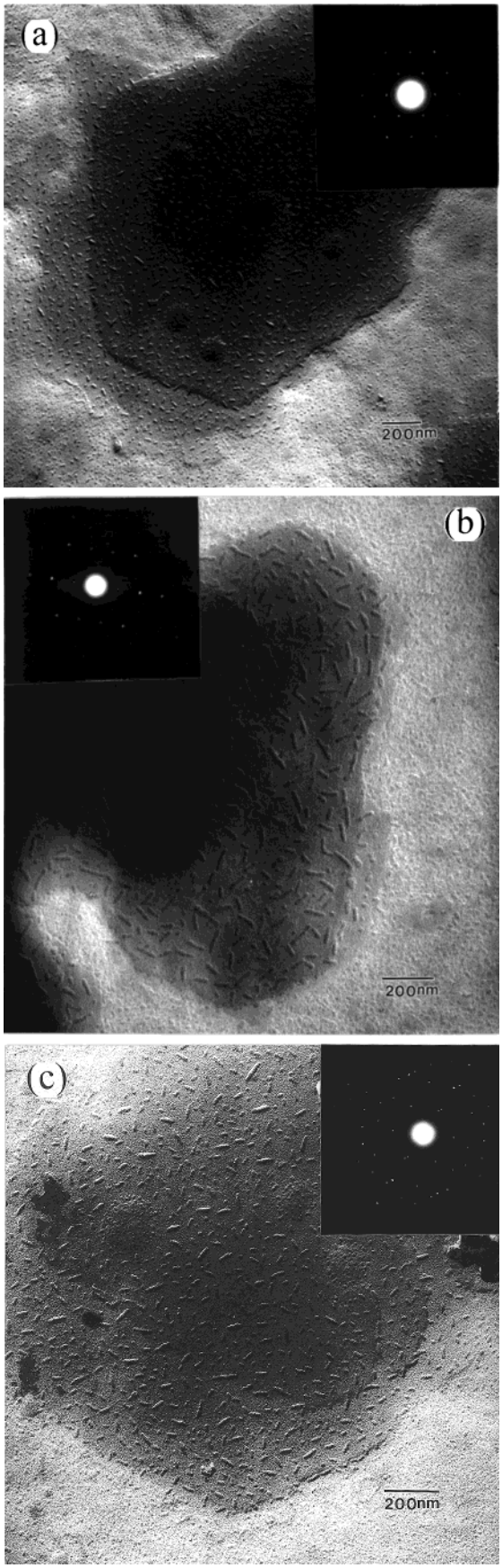

Figure 10. TEM micrographs of (a) decorated α″ crystals crystallized at 260 °C from the melt, (b) decorated *β*′ crystals crystallized at 260 °C from the melt, and (c) decorated coexistent crystals of model I crystallized at 260 °C from the melt. The inset pictures show the corresponding ED patterns originated from the central area of the micrographs and shown with the correct orientation.

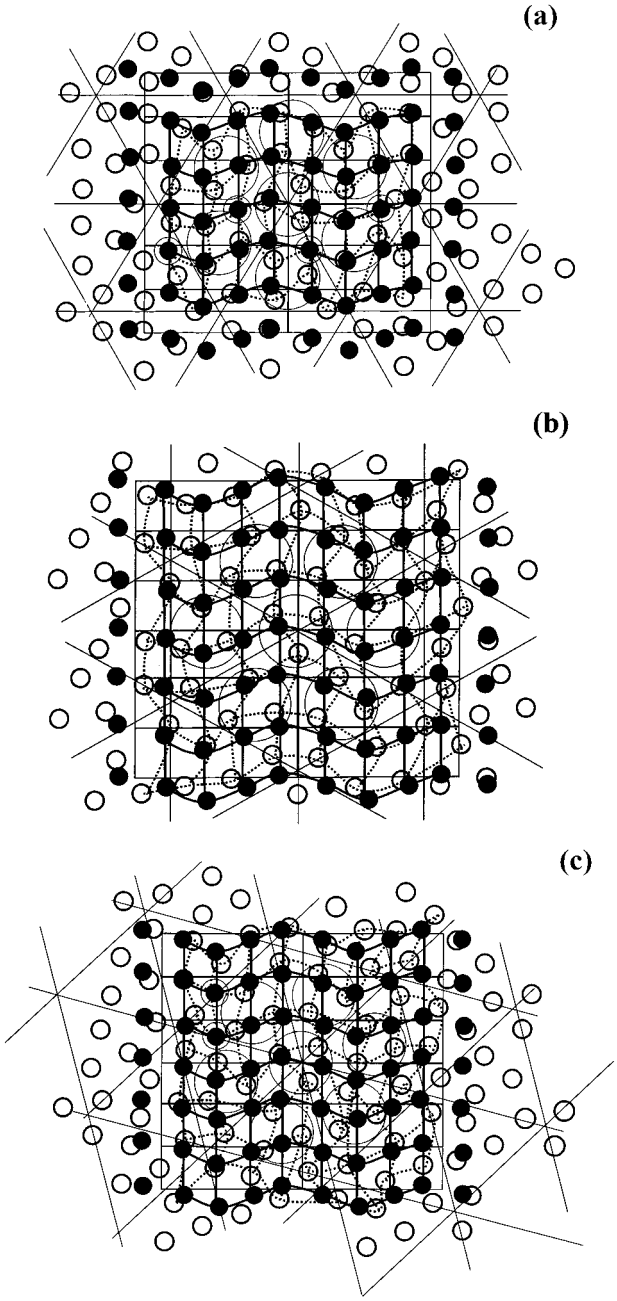

Figure 11. Schematic representation of the rearrangement of molecular chain upon transformation for (a) model I, (b) model II, and (c) model III of the coexistent α″ and *β*′ single crystal.

along the (1*k*0) reflections in the [001] zonal ED pattern. These results are similar to the occurrence of streaks in the ED patterns of syndiotactic polypropylene.[35] Certainly, there have been different interpretations regarding the origins of the formation of streak proposed by other authors in the past.[11−13,36] Among them, the most plausible explanation is to refer the streaks as the results of stacking fault influences where the attachment of a new polymer stem onto the lateral growth face which is not parallel to the *bc*-plane so as to produce irregular fold surfaces of the single crystals.[11] This proposed mechanism may be the true origin of the formation of these diffraction streaks in model II as illustrated in Figure 11b. For model III, a distinct alignment result as compared to models I and II is found. The lattice networks between the α″ and *β*′ crystals are very difficult to align well with each other

as an example illustrated in Figure 11c. There is always a certain amount of molecular chains in the lattice being significantly deviated from the possible lattice point positions for the rearrangement. In fact, the proposed packing model is consistent with the observations of various small deviations to the average examined interangle between the diffraction vectors of (0*k*0) reflections in model III. We suggest that the uncertainty in crystallographic correlation between the α″ and *β*′ phase in the model III is ascribed to the mismatching of molecular rearrangement for lattice adjustment in the proposed model.

There were many studies about the phase transformation for different polymeric materials. The majority of transformations studied was carried out during heating. The temperature changes usually account for the transformation where the energy barrier to transforming the original conformation to the new state is overcome by the changes. The energy barrier can be calculated from conformational analysis and molecular simulation technique. In contrast to the behavior of transformation during heating, the driving forces of the α″ → *β*′ phase transformation for sPS polymorphism in the stage of isothermal crystallization are unascertained. Furthermore, the change of lamellar habit from the hexagonal α″ phase to the elongated hexagonal *β*′ phase during the transition is abnormal. We speculate that the unusual behavior in the morphological change may be attributed to the characteristics of thin films. The molecular chains in the thin film samples are much easier to conduct surface reorganization so as to form regularly faceted changes on the single crystals during the transition. Further studies with regard to the energy barrier for the transformation of sPS polymorphism are necessary in order to evaluate the possible mechanisms for the transition in detail.

Conclusion

Isothermal crystallization-induced α″ → *β*′ phase transformation in sPS polymorphism has been identified in terms of structural analysis for bulk and thin film samples in this study. The observed isothermal transformation is consistent with the predicted results based on the behavior of phase stability inversion. Contrary to crystallization-induced transformation in other polymorphic materials, the isothermal transformation of sPS polymorphism is found to occur after complete crystallization as evidenced by the results of DSC enthalpic measurements. The studies on the crystallographic textures of the coexistent α″ and *β*′ single crystals indicates that the growth of the *β*′ single crystals is on the surface of the α″single crystals in terms of lamellar thickening process so as to form the dual-layer morphology. The lamellar crystals of both phases are grown as flat-on type and possess a common *c*-axis in the crystal structures during the transition. The specific crystallographic correlation in structure gives rise to three different dispositions with respect to the *ab*-planes of the coexistent polymorphic structures. We propose that the transformation is attributed to the characteristic chain packing, the floating chain assembly, in the superstructure-like crystals of sPS. Corresponding molecular movements during the transitions were proposed in terms of the alignment of polymorphic lattice networks.

Acknowledgment. The financial support of the National Science Council (Grant NSC 89-2216-E-005-005) is acknowledged. The authors thank Dr. S. Z. D. Cheng of Institute of Polymer Science of University of Akron and Dr. A. C. Su at Institute of Materials Science and Engineering of National Sun Yet-Sen University (NSYSU) for their helpful discussion. R.M.H. also thanks Ms. S.-Y. Lee of the Regional Instruments Center at NSYSU for her help with the WAXD experiments. We also thank Ms. P.-C. Chao of the Regional Instruments Center at NCHU for her help with the ED experiments.

References and Notes

(1) Guerra, G.; Vitagliano, V. M.; De Rosa, C.; Petraccone, V.; Corradini, P. *Macromolecules* **1990**, *23*, 1539.
(2) Guerra, G.; De Rosa, C.; Vitagliano, V. M.; Petraccone, V.; Corradini, P. *J. Polym. Sci., Part B: Polym. Phys.* **1991**, *29*, 265.
(3) De Rosa, C.; Guerra, G.; Petraccone, V.; Corradini, P. *Polym. J.* **1991**, *23*, 1435.
(4) De Rosa, C.; Rapacciuolo, M.; Guerra, G.; Petraccone, V.; Corradini, P. *Polymer* **1992**, *33*, 1423.
(5) Auriemma, F.; Petraccone, V.; Dal Poggetto, F.; De Rosa, C.; Guerra, G.; Manfredi, C.; Corradini, P. *Macromolecules* **1993**, *26*, 3772.
(6) Chatani, Y.; Shimance, Y.; Ijitsu, T.; Yukinari, T. *Polymer* **1993**, *34*, 1625.
(7) Manfredi, C.; Guerra, G.; De Rosa, C.; Busico, V.; Corradini, P. *Macromolecules* **1995**, *28*, 6508.
(8) De Rosa, C. *Macromolecules* **1996**, *29*, 8460.
(9) Greis, O.; Xu, Y.; Asano, T.; Petermann, J. *Polymer* **1989**, *30*, 590.
(10) Pradere, P.; Thomas, E. L. *Macromolecules* **1990**, *23*, 4954.
(11) Tosaka, M.; Hamada, N.; Tsuji, M.; Kohjiya, S.; Ogawa, T.; Isoda, S.; Kobayashi, T. *Macromolecules* **1997**, *30*, 4132.
(12) Hamada, N.; Tosaka, M.; Tsuji, M.; Kohjiya, S.; Katayama, K. *Macromolecules* **1997**, *30*, 6888.
(13) Tosaka, M.; Hamada, N.; Tsuji, M.; Kohjiya, S. *Macromolecules* **1997**, *30*, 6592.
(14) Cartier, L.; Okihara, T.; Lotz, B. *Macromolecules* **1998**, *31*, 3303.
(15) Conti, G.; Santoro, E.; Resconi, L.; Zerbi, G. *Mikrochim. Acta, Appl. Spectrosc.* **1989**, *1*, 297.
(16) Niquist, R. A. *Appl. Spectrosc.* **1989**, *43*, 440.
(17) Reynolds, N. M.; Savage, J. D.; Hsu, S. L. *Macromolecules* **1989**, *22*, 2867.
(18) Kobayashi, M.; Nakaoki, T.; Ishihara, N. *Macromolecules* **1990**, *23*, 78.
(19) Vittora, V. *Polym. Commun.* **1990**, *31*, 263.
(20) Reynolds, N. M.; Hsu, S. L. *Macromolecules* **1990**, *23*, 3463.
(21) Reynolds, N. M.; Stidham, H. D.; Hsu, S. L. *Macromolecules* **1991**, *24*, 3662.
(22) Rastogi, S.; Gupta, V. D. *J. Macromol. Sci., Phys.* **1994**, *B33*, 129.
(23) Musto, P.; Tavone, S.; Guerra, G.; De Rosa, C. *J. Polym Sci., Part B: Polym. Phys.* **1997**, *35*, 1055.
(24) Grassi, A.; Longo, P.; Guerra, G. *Makromol. Chem., Rapid Commun.* **1989**, *10*, 687.
(25) Gomez, M. A.; Tonelli, A. E. *Macromolecules* **1990**, *23*, 3385.
(26) Capitani, D.; Segre, A. L.; Grassi, A.; Sykora, S. *Macromolecules* **1991**, *24*, 623.
(27) Capitani, D.; De Rosa, C.; Ferrando, A.; Grassi, A.; Segre, A. L. *Macromolecules* **1992**, *25*, 3874.
(28) Keller, A.; Cheng. S. Z. D. *Polymer* **1998**, *39*, 4461.
(29) Ostwald, W. Z. *Phys. Chem.* **1897**, *22*, 286.
(30) Gutzow, I.; Toschew, S. *Krist. Tech.* **1968**, *3*, 485.
(31) Ho, R.-M.; Lin, C.-P.; Tsai, H.-Y.; Woo, E.-M. *Macromolecules* **2000**, *33*, 6517.
(32) Wittmann, J.-C.; Lotz, B. *Makromol. Chem., Rapid Commun.* **1982**, *3*, 733.
(33) Wittmann, J.-C.; Lotz, B. *J. Polym. Sci., Polym. Phys. Ed.* **1985**, *23*, 205.
(34) Corradini, P.; De Rosa, C.; Guerra, G.; Napolitano, R.; Petraccone, V.; Pirozzi, B. *Eur. Polym. J.* **1994**, *30*, 1173.
(35) Bu, Z.; Yoon, Y.; Ho, R. M.; Zhou, W.; Jangchud, I.; Eby, R. K.; Cheng, S. Z. D. *Macromolecules* **1996**, *29*, 6575.
(36) Pradere, P.; Thomsa, E. L. *Macromolecules* **1990**, *23*, 4954.

MA010628+